Quantum transport in non-Markovian dynamically disordered photonic lattices

Ricardo Román-Ancheyta [1,*], Barış Çakmak [2], Roberto de J. León-Montiel [3], and Armando Perez-Leija [4,5]

[1]*Instituto Nacional de Astrofísica, Óptica y Electrónica, Calle Luis Enrique Erro 1, Santa María Tonantzintla, CP 72840, Puebla, Mexico*
[2]*College of Engineering and Natural Sciences, Bahçeşehir University, Beşiktaş, Istanbul 34353, Turkey*
[3]*Instituto de Ciencias Nucleares, Universidad Nacional Autónoma de México, Apartado Postal 70-543, 04510 Ciudad de México, Mexico*
[4]*Max-Born-Institut, Max-Born-Straße 2A, 12489 Berlin, Germany*
[5]*AG Theoretische Optik & Photonik, Institut für Physik, Humboldt-Universität zu Berlin, Newtonstraße 15, 12489 Berlin, Germany*

We show theoretically that the dynamics of a driven quantum harmonic oscillator subject to nondissipative noise is formally equivalent to the single-particle dynamics propagating through an experimentally feasible dynamically disordered photonic network. Using this correspondence, we find that noise-assisted energy transport occurs in this network and if the noise is Markovian or delta correlated, we can obtain an analytical solution for the maximum amount of transferred energy between all network's sites at a fixed propagation distance. Beyond the Markovian limit, we further consider two different types of non-Markovian noise and show that it is possible to have efficient energy transport for larger values of the dephasing rate.

I. INTRODUCTION

From a practical point of view, decoherence (the irreversible loss of quantum coherence) is a multifaceted process which presents advantages and disadvantages depending on the particular circumstances and application. For instance, from the perspective of perfect state transport, decoherence is the obstacle to overcome since it may destroy the states way before they can be conveyed [1]. In contrast, to perform highly efficient energy transport protocols, decoherence has been found to be the best allied [2,3]. Thus, a good understanding of the impact of decoherence on energy transport and energy conversion in the quantum and classical regimes is essential to design functional technologies based on hybrid systems [4], ranging from quantum information processing tasks to quantum thermodynamics applications [5–8].

In optics, one can use integrated photonic devices, e.g., based on direct laser-writing coupled-waveguide lattices [9,10], to study coherent energy transport [11–13], which is an important ingredient in the development of integrated photonic quantum technologies [14,15]. Such devices constitute a well-established, popular, and relatively-low-cost platform among experimentalists due to their practical fabrication process, where their physical and novel geometric properties can be easily tailored [16]. In general, these devices are never completely isolated from their environment; therefore, to describe their energy losses and decoherence processes, a treatment based on the theory of open or stochastic quantum systems [17] is needed.

In the present work we study coherent and incoherent energy transport in a particular type of integrated photonic device termed a Glauber-Fock (GF) photonic lattice [18,19]. We choose this particular photonic structure because its *closed* dynamics is effectively described by the unitary evolution of a displaced quantum harmonic oscillator [18], as experimentally demonstrated in [20,21]. In addition, the physics of nonlinear [22] and non-Hermitian systems [23,24] can also be studied using such photonic devices. Thus far, there is a lack of theory accounting for the interaction of GF lattices with nondissipative noisy environments. Here we close this gap by considering specific instances of Markovian (white) and non-Markovian (correlated) noise. Further, we show that the corresponding *open* system dynamics is equivalent to that of a single excitation propagating in a dynamically disordered network. Such noisy scenarios are quite relevant in integrated photonics. For example, the interplay between noise and interference effects can lead to a faster transmission in the transport dynamics of integrated photonic mazes [25] or enhancing the coherent transport using controllable decoherence [12]. Our results also present a clear manifestation of the so-called environment-assisted transport phenomenon in the single-excitation regime [2,3,26–28]. Furthermore, we observe that non-Markovianity in the dynamics of the system enhances the range of dephasing rates over which this effect persists in our model.

The paper is structured as follows. In Secs. II and III we analytically show that the master equation governing the closed and open dynamics of a single excitation in a GF lattice is identical to the one describing the evolution of a driven quantum harmonic oscillator. We then examine the impact of nondissipative Markovian noise on the energy transport. In Sec. IV we explore non-Markovian noise models, while in Sec. V we discuss the usefulness of having a correspondence between the master equations of a driven harmonic oscillator and a single particle propagating in a GF lattice. In particular, when the noise-assisted energy transport phenomenon is manifested in the Markovian case, it is possible to find an analytical solution for the maximum amount of energy transferred between all sites of the photonic network. This

*ancheyta6@gmail.com

constitutes one of the main results of the present work and provides a clear advantage in energy transport calculations. For the non-Markovian case, we find a substantial increase in the range of the dephasing rate for which the noise-assisted transport takes place, indicating that the common idea [29] that noise-assisted transport occurs only in the moderate decoherence regime is no longer accurate when the environment's finite correlation time is considered. In Sec. VI we summarize and discuss our conclusions.

II. GLAUBER-FOCK OSCILLATOR MODEL

We start by introducing the Hamiltonian of the quantum harmonic oscillator (HO) in one dimension driven by an external perturbation $\hat{H} = \hbar\omega\hat{n} + \hbar g(\hat{a} + \hat{a}^\dagger)$ [30]. Here $\hat{a}$ and $\hat{a}^\dagger$ are the usual annihilation and creation operators, $\hat{n} = \hat{a}^\dagger\hat{a}$ is the number operator, and ω is the oscillator frequency. The term $\hbar g(\hat{a} + \hat{a}^\dagger)$ represents a displacement with strength g. In the field of integrated photonics, this Hamiltonian governs the light dynamics in the so-called Glauber-Fock lattice [18,20,21] or GF oscillator.

A. Unitary dynamics in GF lattices

Assume that the state of the driven HO is given by $|\Psi(t)\rangle = \sum_m \mathcal{A}_m(t)|m\rangle$, with $|m\rangle$ the energy eigenstates and $\mathcal{A}_m(t)$ the corresponding probability amplitudes. Then it is possible to show that the equations of motion for $\mathcal{A}_m(t)$, dictated by the time-dependent Schrödinger equation $i\hbar\frac{d}{dt}|\Psi(t)\rangle = \hat{H}|\Psi(t)\rangle$ with the above-mentioned Hamiltonian, are isomorphic to the ones describing the dynamics of a mode field amplitude $\mathcal{E}_m(z)$ propagating in a high-quality optical waveguide that is coupled evanescently to its nearest neighbors forming a semi-infinite photonic lattice given as [21]

$$i\frac{d}{dz}\mathcal{E}_m(z) + \mathcal{C}_m\mathcal{E}_{m-1}(z) + \mathcal{C}_{m+1}\mathcal{E}_{m+1}(z) + \alpha m\mathcal{E}_m(z) = 0, \tag{1}$$

where z represents the propagation coordinate; $\mathcal{C}_m \equiv \mathcal{C}_1\sqrt{m}$ are the nonuniform coupling coefficients, with $\mathcal{C}_1$ the coupling between the zeroth and the first waveguide; and αm are the propagation constants. Importantly, in the context of photonic lattices, the term αm implies that the refractive index of the waveguides describes a potential that is gradually increasing (for $\alpha > 0$) with the waveguide number. That is, the potential describes a ramp whose slope is controlled by the parameter α (see Fig. 1 of [21] for an illustration of this refractive index profile). In a GF lattice α can also be negative, generating a different lattice response. However, throughout this work we assume that α is always positive. The correspondence between Eq. (1) and the equations of $\mathcal{A}_m(t)$ can be established if we identify the label m of each excited waveguide with the corresponding Fock state $|m\rangle$, $\mathcal{C}_1$ with g, α with ω, and the propagation coordinate z with the time variable t [31]. The probability distribution $P_m(t) = |\mathcal{A}_m(t)|^2$ of the quantum system represents the intensity distribution $I_m(z) = |\mathcal{E}_m(z)|^2$ of the light in the photonic array. Details for fabricating this type of waveguide system can be found in [21]. For instance, to achieve the increasing coupling $\mathcal{C}_1\sqrt{m}$ between the neighboring waveguides, these need to be directly inscribed in a
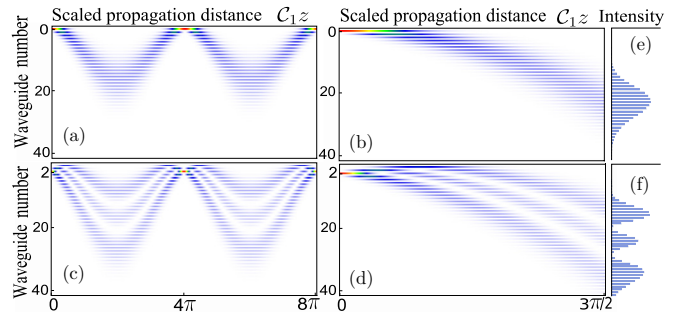

FIG. 1. Light intensity propagation in a photonic lattice obtained by integrating Eq. (1). Light is initially launched into a single waveguide labeled as (a) and (b) $m = 0$ and (c) and (d) $m = 2$. In (e) and (f) we show the output light intensity $I_m(Z) = |\mathcal{E}_m(Z)|^2$ at $Z = 3\pi/2$ for the simulations presented in (b) and (d), respectively. Note that $Z \equiv \mathcal{C}_1 z$ is the scaled propagation distance. Here $I_m(Z)$ exhibits m nodes, as expected from the probability distribution of the nonclassical displaced Fock states [20]. When the ramping potential is activated, $\alpha \neq 0$, we see Bloch-like oscillations [32] (left), where the light exhibits revivals every period $Z_{\text{rev}} = 2\pi k\mathcal{C}_1/\alpha$, with k an integer [21]. We have set the ratio (a) and (c) $\alpha/\mathcal{C}_1 = 1/2$ and (b) and (d) $\alpha/\mathcal{C}_1 = 0$, which are feasible experimental values that would allow us to implement realistic integrated photonic devices occupying few centimeter-scale footprints (see the text for more details).

polished fused silica glass using femtosecond-laser-writing technology [9] with a decreasing separation distance between them, $d_m = d_1 - (s/2)\ln m$, where d_1 and s are parameters of $\mathcal{C}_1$ that depend on the corresponding waveguide width and the optical wavelength. With this configuration the evanescent couplings $\mathcal{C}_m = \mathcal{C}_1 \exp(-[d_m - d_1]/s)$ satisfy the desired square root distribution.

Figure 1 depicts the intensity propagation in a GF lattice of 40 waveguides emulating the unitary evolution of the driven quantum harmonic oscillator. Clearly, we see two scenarios where the light spreads over the entire photonic array (delocalization) [20] and another in which it strongly localizes as a manifestation of the so-called Bloch-like oscillations [32]. The analytical solution of Eq. (1) can be found in Ref. [21] in terms of the associated Laguerre polynomials. As a function of the scaled (or normalized) distance $Z \equiv \mathcal{C}_1 z$, the behavior of $\mathcal{E}_m(Z)$ simply depends on the ratio $\alpha/\mathcal{C}_1$, and the so-called revival distance Z_{rev} is given as $Z_{\text{rev}} = 2\pi k\mathcal{C}_1/\alpha$. Note that the difference in the case $\alpha > \mathcal{C}_1$ as compared to $\alpha < \mathcal{C}_1$ is the period of the Bloch-like oscillations, which is short in the former case. Here, to be in accordance with the reported experimental values of α and $\mathcal{C}_1$ in previous works, we adopt the latter case. These are simple examples showing the typical dynamics of coherent energy transport in closed systems where strong interference effects dominate. However, when dynamical disorder mechanisms are considered in an open system description, a more involved study of the incoherent energy transport dynamics is necessary, which we aim to cover in the following sections.

B. Open dynamics: Markovian master equation

Under the action of Markovian dephasing, the density matrix $\hat{\rho}$ of the harmonic oscillator described by the Hamiltonian

$\hat{H} = \hbar\omega\hat{n} + \hbar g(\hat{a} + \hat{a}^\dagger)$ obeys the phenomenological master equation $d\hat{\rho}/dt = -i[\hat{H}, \hat{\rho}] + \gamma\hat{\mathcal{L}}[\hat{n}]\hat{\rho}$. Here the second term on the right-hand side is the standard Lindblad superoperator given by $\hat{\mathcal{L}}[\hat{x}]\hat{\rho} \equiv \hat{x}\hat{\rho}\hat{x}^\dagger - \frac{1}{2}(\hat{x}^\dagger\hat{x}\hat{\rho} + \hat{\rho}\hat{x}^\dagger\hat{x})$, with γ the constant dephasing rate. This master equation can be derived using standard techniques of open quantum systems, where the usual Born and Markov approximations are used [17].

In general, pure dephasing processes are energy preserving [33]; as a result, the interaction between the system and its environment commutes with the unperturbed Hamiltonian of the system, $\omega\hat{n}$ in the present case. To obtain the master equation we compute the matrix elements $\langle n|\hat{H}\hat{\rho}|m\rangle = \omega n \rho_{nm} + \sum_r gV_{nr}\rho_{rm}$, with $V_{rm} \equiv \langle r|(\hat{a} + \hat{a}^\dagger)|m\rangle = (\sqrt{m}\delta_{rm-1} + \sqrt{m+1}\delta_{rm+1})$; a similar expression is obtained for $\langle n|\hat{\rho}\hat{H}|m\rangle$. The matrix elements for the dephasing term are

$$\gamma\langle n|\hat{\mathcal{L}}[\hat{n}]\hat{\rho}|m\rangle = \sqrt{\gamma}n\sqrt{\gamma}m\rho_{nm} - \rho_{nm}(\gamma n^2 + \gamma m^2)/2. \quad (2)$$

Therefore, we obtain

$$i\frac{d}{dt}\rho_{nm} = \left[(\omega n - \omega m) - \frac{i}{2}(\gamma n^2 + \gamma m^2)\right]\rho_{nm} + i\sqrt{\gamma}n\sqrt{\gamma}m\rho_{nm} - \sum_r gV_{rm}\rho_{nr} + \sum_r gV_{nr}\rho_{rm}. \quad (3)$$

Defining the variables $\omega_n \equiv n\omega$, $\gamma_n \equiv \gamma n^2$, and $v_{ij} \equiv gV_{ij}$, we can rewrite Eq. (3) as

$$i\frac{d}{dt}\rho_{nm} = \left[(\omega_n - \omega_m) - \frac{i}{2}(\gamma_n + \gamma_m)\right]\rho_{nm} + i\sqrt{\gamma_n\gamma_m}\rho_{nm} - \sum_r v_{rm}\rho_{nr} + \sum_r v_{nr}\rho_{rm}, \quad (4)$$

which is the same master equation that a single particle, or excitation, follows during its time evolution in a quantum network affected by nondissipative noise, as we show in the following section [see also Eq. (1) of Ref. [34]]. Since Eq. (4) describes a pure-dephasing process, only the off-diagonal matrix elements of $\hat{\rho}$ are affected by the constant dephasing rate γ. Notice that the form of $\gamma_n \equiv \gamma n^2$ implies that Fock states with high n are more severely affected by dephasing.

III. SINGLE-PARTICLE DYNAMICS IN A NETWORK AFFECTED BY MARKOVIAN NOISE

In this section we show the equivalence between Eq. (3) [or alternatively Eq. (4)] and the master equation governing the evolution (or propagation) of a single particle in a tight-binding quantum network composed of N coupled sites affected by a stochastic nondissipative noise (pure dephasing). In the following and throughout the whole paper, keep in mind that with the correspondence between the spatial (z) and temporal (t) variables, the integrated photonic lattices discussed in the preceding section would be a particular case of such networks. In order to establish this connection we begin by writing the single-particle tight-binding Hamiltonian

$$\hat{H}_S = \sum_{n=1}^N \omega_n(t)|n\rangle\langle n| + \sum_{j<n}^N \kappa_{jn}(|j\rangle\langle n| + |n\rangle\langle j|) \quad (5)$$

such that the evolution of the single-particle wave function ψ_n at the nth site is governed by the stochastic Schrödinger equation

$$\frac{d\psi_n}{dt} = -i\omega_n(t)\psi_n - i\sum_{j\neq n}\kappa_{nj}\psi_j, \quad (6)$$

where κ_{nj} represents, in principle, an arbitrary hopping rate between sites n and j. In addition, $\omega_n(t) = n[\omega + \phi_n(t)]$ is the frequency at the nth site that is affected by the random fluctuations $\phi_n(t)$. Note that each site exhibits a different natural frequency that changes linearly with n, namely, ωn. In most of the literature dealing with stochastic quantum networks, all sites have the same frequency. However, since our main goal is to establish a connection between the present physical setting and the one describing a driven HO, outlined in Sec. II B, we choose the frequency of the nth site to be proportional to n. To introduce pure dephasing we consider $\phi_n(t)$ to be a Gaussian stochastic process with a zero mean $\langle\phi_n(t)\rangle = 0$ and two-point correlation function given as

$$\langle\phi_n(t)\phi_m(t')\rangle = \Gamma\delta_{nm}\delta(t-t'), \quad (7)$$

where Γ is the noise strength (dephasing rate) that we have assumed to be the same for all sites. The Kronecker delta δ_{nm} implies that the noise is uncorrelated between sites n and m, the Dirac delta function $\delta(t-t')$ describes the Markovian nature (white noise) of the stochastic process, and $\langle\cdots\rangle$ denotes the average over all possible noise realizations. Next, following Ref. [35], we derive the corresponding master equation for the density matrix

$$i\frac{d}{dt}\sigma_{nm} = \left[(n\omega - m\omega) - \frac{i}{2}(\Gamma n^2 + \Gamma m^2)\right]\sigma_{nm} + i\sqrt{\Gamma}n\sqrt{\Gamma}m\delta_{nm}\sigma_{nm} - \sum_j \kappa_{jm}\sigma_{nj} + \sum_j \kappa_{nj}\sigma_{jm}, \quad (8)$$

where $\sigma_{nm}(t) \equiv \langle\psi_n\psi_m^*\rangle$ (see Appendix A). Adopting the notation $\omega_n = n\omega$ and $\Gamma_n = \Gamma n^2$, we obtain

$$i\frac{d}{dt}\sigma_{nm} = \left[(\omega_n - \omega_m) - \frac{i}{2}(\Gamma_n + \Gamma_m)\right]\sigma_{nm} + i\sqrt{\Gamma_n\Gamma_m}\delta_{nm}\sigma_{nm} - \sum_j \kappa_{jm}\sigma_{nj} + \sum_j \kappa_{nj}\sigma_{jm}. \quad (9)$$

Notice that the only difference between Eqs. (9) and (4) is the Kronecker delta δ_{nm} appearing in the second term on the right-hand side of Eq. (9). This difference emerges from the fact that we have assumed no correlation between noise affecting different sites [see Eq. (7)]. However, Eqs. (4) and (9) become identical [no Kronecker delta in Eq. (9)] if we assume that $\langle\phi_n(t)\phi_m(t')\rangle = \Gamma\delta(t-t')$, i.e., there must be a correlation between stochastic processes at different sites.

Such a correlation condition, which at first glance seems unlikely to be achieved in practice, can easily be emulated using laser-written photonic lattices in which temporal correlations are translated into longitudinal spatial correlations. In these photonic devices, ultrashort laser pulses are used to inscribe each waveguide (site) with a customized refractive index (propagation constant or site energy) depending
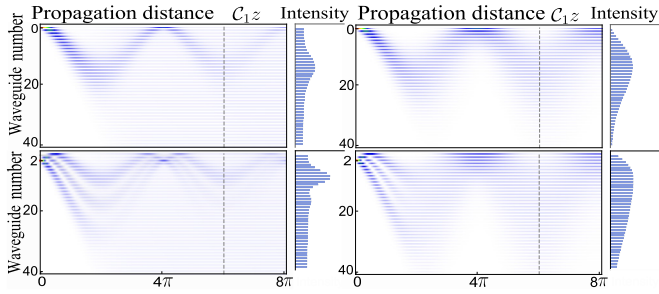
FIG. 2. Light propagation in a dynamically disorder Glauber-Fock lattice. On the left we see the diagonal elements σ_{nn} obtained by numerical integration of Eq. (9) describing the emerging intensity distribution in the lattice; on the right we depict the matrix elements ρ_{nn} from Eq. (4). For these simulations we used the same parameters and initial conditions as for Figs. 1(a) and 1(c) but now adding white noise with a dephasing rate $\Gamma = 0.001$ (left) and $\gamma = 0.025$ (right). Due to the noise, light starts to delocalize and the effect is more prominent in the regions where complete Bloch-like oscillations would appear in the absence of noise (see Fig. 1). The vertical dashed line indicates the distance at which the light intensity is calculated.

on the writing speed [34]. The random fluctuations (noise) in the refractive index are implemented by modulating the laser's writing speed during the manufacturing process with a high degree of control, keeping the coupling coefficients unchanged [25]. Contrary to uncorrelated noise (7), where independent noise generators in each inscribed waveguide are used [25,34], for correlated noise between sites ($\delta_{nm} = 1$), a single generator would need to be used during each fabrication step of the waveguide array.

Let us emphasize that in GF lattices, the hopping rates must satisfy, as in the previous case, $\kappa_{nj} = g(\sqrt{j}\delta_{nj-1} + \sqrt{j+1}\delta_{nj+1})$ and the time evolution must be interpreted as spatial propagation. The light intensity represents the probability distribution P_n, but now this is given by the diagonal matrix elements ρ_{nn} and σ_{nn}.

In Fig. 2 we compare the dynamics generated by numerically integrating Eqs. (9) and (4). Specifically, we present the corresponding diagonal elements σ_{nn} and ρ_{nn} to illustrate the intensity propagation in a dynamically disorder Glauber-Fock photonic lattice. Both master equations were numerically solved using the technique described in [36]. In Fig. 2 one can see that, due to the added noise, near the revival distances $\mathcal{C}_1 z_{\text{rev}} = 4\pi k$, light delocalization is more prominent. From the experimental point of view this means that one could build photonic waveguide arrays having just one Bloch-like oscillation ($k = 1$) and see the desired dephasing effect. In fact, the ratio $\alpha/\mathcal{C}_1 = 1/2$ used in Figs. 1 and 2 can easily be obtained by choosing the coupling between the zeroth and the first waveguide as $\mathcal{C}_1 = 0.88$ cm^{-1} [37,38] and $\alpha = 0.044$ mm^{-1} [32]. The use of these values implies that we should design approximately 40 nearest-neighbor coupled waveguides with $z_{\text{rev}} = 4\pi/\mathcal{C}_1 = 14.28$ cm, which is a feasible scenario. For instance, in [11,12,20,21,39] 10- to 15-cm-long waveguide arrays were built, and in [37,38], 101 identical waveguides were inscribed within one of these types of arrays. In the photonic device, the parameter $\mathcal{C}_m = \mathcal{C}_1\sqrt{m}$ increases with the waveguide's label, and by using the above parameters we

obtain $\mathcal{C}_{40} \approx 5.5$ cm^{-1}, which corresponds to the largest coupling coefficient reported experimentally in [40]. It is worth pointing out that, given the stochastic nature of the process, a certain number of waveguide samples is needed in order to observe the mean density matrix described in Eq. (9). Previous work by two of us [34] has shown that this number is approximately 20. We would also like to mention that reconfigurable electrical oscillator networks [27,41] and optical tweezer arrays [42,43] are other viable experimental platforms in which Eq. (9) and the correlated noise condition between different sites can be realized.

IV. TIME-DEPENDENT DEPHASING RATE IN THE MASTER EQUATION

We now turn our attention to generalize the results obtained in the preceding section to the case of time-dependent dephasing. This opens up the possibility to introduce memory effects in the dynamics of both models, that is, it enables investigations of non-Markovian effects.

A. Glauber-Fock oscillator

The master equation, in the Lindblad form, for the Hamiltonian $\hat{H}$ under a time-dependent dephasing noise is given as

$$\frac{d\hat{\rho}}{dt} = -i[\hat{H}, \hat{\rho}] + \gamma(t)\hat{\mathcal{L}}[\hat{n}]\hat{\rho}. \tag{10}$$

This equation is an *ad hoc* generalization of the master equation of a two-level system describing pure-dephasing dynamics in a possibly non-Markovian regime [see Eq. (9) of Ref. [44] and Eq. (17) of Ref. [45]]. In cases where $\gamma(t)$ becomes negative, the quantum dynamical semigroup property of Eq. (10) no longer holds [17]. Consequently, the divisibility of the quantum map is broken and Eq. (10) can be classified as non-Markovian [45,46]. Here we only consider cases in which $\gamma(t)$ is non-negative. However, it is worth pointing out that Eq. (10) can be used to describe the dynamics of the system under non-Markovian environments provided the dephasing rates exhibit finite environment correlation times [44,47].

From Eq. (10), and following the same steps as in the preceding section, we obtain the master equation

$$i\frac{d}{dt}\rho_{nm} = \left[(\omega_n - \omega_m) - \frac{i}{2}[\gamma_n(t) + \gamma_m(t)]\right]\rho_{nm}$$
$$+ i\sqrt{\gamma_n(t)\gamma_m(t)}\rho_{nm} - \sum_r \kappa_{rm}\rho_{nr} + \sum_r \kappa_{nr}\rho_{rm}. \tag{11}$$

It is interesting to note that the only difference between this expression and Eq. (4) is the time-independent γ_n, which is now replaced by $\gamma_n(t) \equiv \gamma(t)n^2$. In what follows, we discuss its effect in the transport dynamics of complex quantum networks.

B. Single-particle dynamics in a quantum network

We start by investigating the dynamics of a single particle under the influence of a Gaussian non-Markovian stochastic noise $\Omega_n(t)$, with zero mean $\langle\Omega_n(t)\rangle = 0$ and two-point cor-

relation function

$$2\langle\Omega_n(t)\Omega_m(t')\rangle = \Gamma\lambda\delta_{nm}e^{-\lambda|t-t'|}. \qquad (12)$$

This is the well-known modified Ornstein-Uhlenbeck noise, where Γ is the inverse relaxation time and λ is the noise bandwidth which is related to the environmental memory time as $\tau_c = \lambda^{-1}$, such that when λ is finite the τ_c is also finite, giving a non-Markovian character to the dynamics [see Eq. (3) of [44] and Eq. (2.9) of Ref. [47] for a detailed discussion on Ornstein-Uhlenbeck noise]. This process has a well-defined Markovian limit which is obtained when $\lim_{\lambda\to\infty}\langle\Omega_n(t)\Omega_m(t')\rangle = \Gamma\delta_{nm}\delta(t-t')$ [44].

As shown in Appendix A, for the present case we obtain the equation

$$\frac{d}{dt}\sigma_{nm} = -i(n\omega - m\omega)\sigma_{nm} - i\sum_{j\neq n}\kappa_{nj}\sigma_{jm} + i\sum_{j\neq m}\kappa_{jm}\sigma_{nj}$$
$$-in\langle\psi_n\psi_m^*\Omega_n(t)\rangle + im\langle\psi_n\psi_m^*\Omega_m(t)\rangle, \qquad (13)$$

where the matrix elements are given as $\sigma_{nm} = \langle\psi_n\psi_m^*\rangle$. Although $\Omega_n(t)$ represents in general non-Markovian noise, it is still a Gaussian process; therefore, we can use Novikov's theorem [48] to compute the elements

$$\langle\psi_n\psi_m^*\Omega_n(t)\rangle \approx -\frac{i}{2}n\sigma_{nm}(t)\Gamma(t) + \frac{i}{2}m\delta_{mn}\sigma_{nm}(t)\Gamma(t), \qquad (14)$$

where $\Gamma(t) \equiv \Gamma(1 - e^{-\lambda t})/2$ is basically the time integral of the two-point correlation function of the environment [44] (see Appendix B for details). Hence, Eq. (13) becomes

$$i\frac{d}{dt}\sigma_{nm} = \left[(\omega_n - \omega_m) - \frac{i}{2}[\Gamma_n(t) + \Gamma_m(t)]\right]\sigma_{nm}$$
$$+ i\sqrt{\Gamma_n(t)\Gamma_m(t)}\delta_{nm}\sigma_{nm} - \sum_r\kappa_{rm}\sigma_{nr} + \sum_r\kappa_{nr}\sigma_{rm}, \qquad (15)$$

where $\Gamma_n(t) \equiv \Gamma(t)n^2$. This is the master equation and describes the dynamics of a single particle in a non-Markovian environment and, as expected, it reduces to Eq. (9) when $\Gamma(t)$ is time independent.

Similarly to the case of Markovian noise, discussed in the preceding section, the only difference between Eqs. (15) and (11) is the additional Kronecker delta appearing in Eq. (15). That is, when there are noise correlations between different sites, ρ_{nm} and σ_{nm} become identical. Even though they exhibit similar evolution, ρ_{nm} and σ_{nm} are of a different nature. In other words, ρ_{nm} is the density matrix for a quantum harmonic oscillator inhabiting an infinite-dimensional Hilbert space spanned by an infinite number of Fock states. In contrast, σ_{nm} is the density matrix of a single particle, or excitation, evolving in a quantum network made out of a finite number of coupled sites, with their corresponding Hilbert space.

Finally, we would like to stress that the derivation of Eqs. (9) and (15) is in principle valid for arbitrary time-independent hopping rates κ_{rm} and not only for nearest-neighbor interactions. Therefore, these master equations may describe an extensive class of complex networks that do not necessarily have to be photonic.

V. AVERAGE ENERGY OF THE SYSTEM

A. Analytical solution for the Markovian case

In this section we discuss some advantages of having a correspondence between the master equations of a driven quantum harmonic oscillator and a single particle propagating in a photonic network. When one is interested in computing the average of certain observables, e.g., the average energy of a particle propagating in a network, solving the HO master equation is much simpler than solving the latter. For example, if we insert the Hamiltonian describing the Glauber-Fock oscillator $\hat{H}_{GF} \equiv \omega\hat{n} + g(\hat{a} + \hat{a}^\dagger)$ into Eq. (10), we readily obtain the equations of motion for the average of the number and field operators

$$\frac{d\langle\hat{n}\rangle}{dt} = -ig\langle\hat{a}^\dagger\rangle + ig\langle\hat{a}\rangle,$$
$$\frac{d\langle\hat{a}\rangle}{dt} = [-i\omega - \gamma(t)]\langle\hat{a}\rangle - ig, \qquad (16)$$

where $d\langle\hat{a}^\dagger\rangle/dt = d\langle\hat{a}\rangle^*/dt$. In the absence of dephasing $\gamma(t) = 0$ and assuming the initial condition $|\psi(0)\rangle = |m\rangle$, these equations reduce to the well-known solution for the average of the number operator $\langle\hat{n}(t)\rangle = m + (2g/\omega)^2\sin^2(\omega t/2)$. From this expression, one can directly determine the time at which the states return to their initial configuration (revival time) $t_{rev} = 2\pi k/\omega$, with k an integer. Further, in the limit $\omega \to 0$, the evolution operator becomes the Glauber displacement displacement operator, $D(\alpha) = \exp(\alpha\hat{a} - \alpha^*\hat{a}^\dagger)$ with $\alpha = igt$, which transforms a vacuum initial state into a coherent state [20]. Accordingly, in this limit we have $\lim_{\omega\to 0}\langle\hat{n}(t)\rangle \sim (gt)^2$, which corresponds to the average value of a coherent state. For the case of nondissipative (pure dephasing) Markovian noise, the dephasing rate is a non-negative constant $\gamma \neq 0$. Then the average for the number operator is

$$\langle\hat{n}(t)\rangle = m + \frac{2g^2}{(\omega^2 + \gamma^2)^2}[f(t) + e^{-\gamma t}g(t)], \qquad (17)$$

where we have defined the functions $f(t) \equiv \gamma^2(\gamma t - 1) + \omega^2(\gamma t + 1)$ and $g(t) \equiv (\gamma^2 - \omega^2)\cos(\omega t) - 2\gamma\omega\sin(\omega t)$. It is remarkable that the temporal behavior of $\langle\hat{n}(t)\rangle$ in the quantum system gives crucial information about the energy transport across all sites in the photonic structure at a fixed propagation distance [31]. This is because $\langle\hat{n}(t)\rangle$ can be rewritten as $\langle\hat{n}(t)\rangle = \sum_n P_n(t)n$, where $P_n(t) = \rho_{nn}(t)$ is the probability distribution that we are associating with the light intensity $I_n(z)$ on each waveguide of the photonic lattice. So, in GF lattices, $I_n(z)$ is measured first and then the quantity $\langle\hat{n}(z)\rangle_{class} \equiv \sum_{m=0}^N mI_m(z)$ is evaluated. This corresponds to the classical analog of the average photon number in waveguide arrays. Evaluating $\langle\hat{n}(t)\rangle$ at the revival time (revival distance in the GF lattice) yields

$$\langle\hat{n}(t_{rev})\rangle = m + \frac{2g^2}{\omega^2}\left[\frac{2\pi k\tilde{\gamma}}{1 + \tilde{\gamma}^2} + \frac{1 - \tilde{\gamma}^2}{(1 + \tilde{\gamma}^2)^2}(1 - e^{-2\pi k\tilde{\gamma}})\right], \qquad (18)$$

where $\tilde{\gamma} = \gamma/\omega$ is the scaled dephasing rate and m is the initially excited site. Note that $\langle\hat{n}(t_{rev})\rangle$ attains its maximum
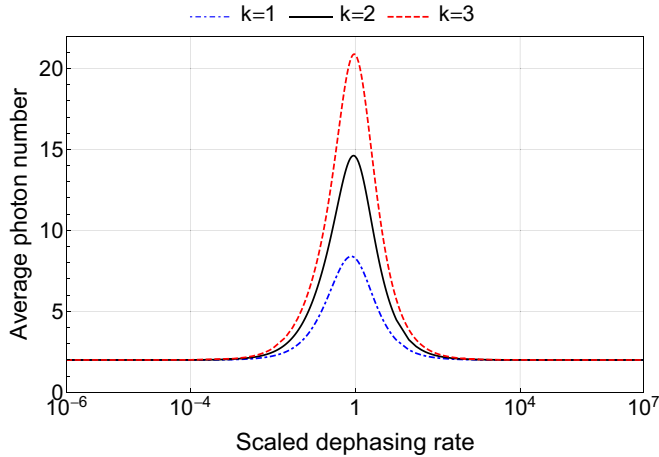
FIG. 3. Manifestation of the noise-assisted transport phenomenon, captured by the average photon number of Eq. (18), as a function of the scaled dephasing rate $\tilde{\gamma} = \gamma/\omega$ at different scaled revivals times counted by k, the ratio $g/\omega = 1$, and the initial condition $m = 2$.

value when the decoherence rate is comparable to the energy scale of the system, i.e., when $\tilde{\gamma} \sim 1$ Eq. (18) reduces to $\langle \hat{n}(t_{\text{rev}}) \rangle_{\text{max}} \sim m + 2\pi k (g/\omega)^2$. This result indicates that independently of the initial condition (excited site) $|m\rangle$, the delocalization of the initial excitation will increase linearly, as a function of k, at each revival time (distance), as shown in Fig. 3.

The Bell-like shape depicted in Fig. 3 is in fact a signature of the so-called environment-assisted transport phenomenon, which in the present case is symmetric with respect to the scaled dephasing rate. Note that this result contrasts with the asymmetric behavior typically observed in other coupled-oscillator systems [26,31,49].

In general, there are two distinct regimes in systems exhibiting noise-assisted transport. For small dephasing rate $\tilde{\gamma} \ll 1$, the energy transport is proportional to $\tilde{\gamma}$ such that Eq. (18) reduces to $\langle \hat{n}(t_{\text{rev}}) \rangle \sim m + 4\pi k (g/\omega)^2 \tilde{\gamma}$. On the other hand, when the dephasing rate is very high $\tilde{\gamma} \gg 1$, the energy transport decreases with $1/\tilde{\gamma}$; in fact, it is easy to show that $\langle \hat{n}(t_{\text{rev}}) \rangle \sim m + 4\pi k (g/\omega)^2 \tilde{\gamma}^{-1}$. These regimes are shown in Fig. 4 (see the black solid lines). The fact that the energy transport has a nonmonotonic behavior can be understood, in a quantum scenario, as a consequence of the quantum Zeno effect (QZE) [50]. In the QZE a frequent measurement on a quantum system inhibits transitions between quantum states [51]. In our system the QZE is dominant when the dephasing rate is extremely high, i.e., when the nondissipative noise acts as the measurement process.

In the corresponding optical context of waveguide arrays, the above effects are expected to occur at the revival distance, under the assumptions of coupling coefficients without disorder and no losses in the waveguide array. However, that is not the case in practical implementations. For example, in the presence of static disorder, Anderson localization of light will occur for large disorder values, as experimentally demonstrated in [38] for $\alpha = 0$, i.e., without Bloch oscillations. When static disorder and Bloch oscillations are both
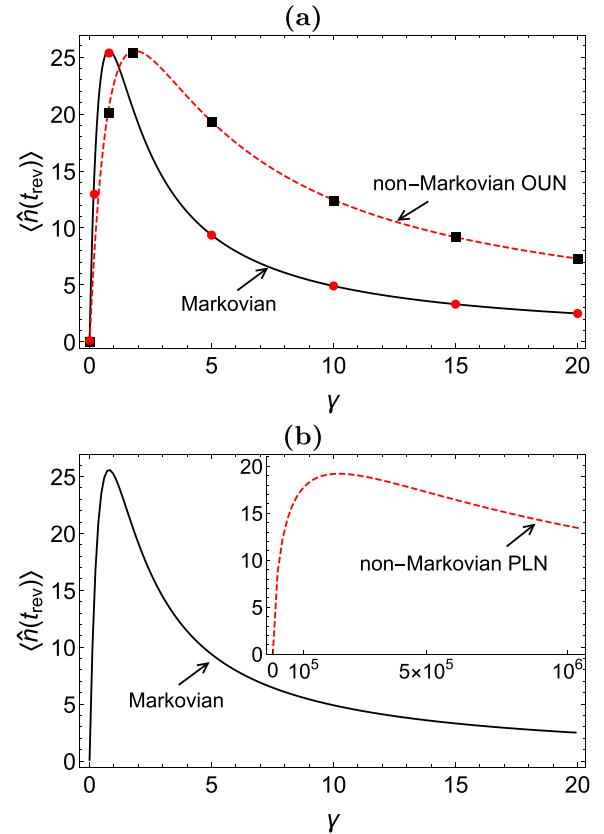

FIG. 4. Noise-assisted transport phenomenon in a Glauber-Fock oscillator (lattice) as a function of the dephasing rate γ under (a) Ornstein-Uhlenbeck noise and (b) power-law noise. The system was prepared initially in ground state $|0\rangle$, i.e., $m = 0$, $g = 1$, $\omega = 0.5$, and $k = 1$. For (a) $\lambda \to \infty$ and (b) $\lambda^{-1} \to \infty$ the black solid line corresponds to the Markovian limit given by Eq. (18) and for (a) $\lambda^{-1} = 10$ and (b) $\lambda = 10$ the red dashed line shows the behavior in the non-Markovian regime evaluating Eq. (16) at t_{rev}. We obtain the red circles and black squares by integrating the master equation (11).

present, hybrid Bloch-Anderson localization of light emerges with gradual washing out of Bloch oscillations [39]. Nevertheless, in such a case, the first Bloch-like revival (the one we have required to be present in this work) is still visible [39]. Hence, we deduce that our results are robust against static disorder. On the other hand, a typical experiment of this kind shows low losses. To be more specific, propagation losses are in the range of 0.1–0.9 dB cm^{-1} for straight sections of the waveguides and also there is an excellent mode overlap with standard fibers (0.1 dB cm^{-1}) [10,16,34]. Moreover, losses are approximately independent of the writing speed [9].

Before concluding this subsection, we would like to point out that while we have assumed zero-temperature conditions for the driven quantum harmonic oscillator, there is no restriction for considering temperature effects upon the photonic lattices structures. Most experiments using direct laser-written waveguides are performed at room temperature [9,10]. Moreover, impressive thermal effects can be admitted on these devices. For instance, in [52] it was experimentally shown that by varying a temperature gradient, the Bloch oscillations'

period and amplitude could be controlled. This can be done by heating and cooling the opposite sides of the waveguide array. Specifically, a transverse linear temperature gradient ΔT leads to a linear variation of the propagation constants, i.e., $\alpha \propto \Delta T$. Such a result suggests an attractive alternative to get the desired ramp potential or the random fluctuations without changing the laser's writing speed.

B. Numerical solution for the non-Markovian case

We now look into the numerical solutions of the equations of motion for the average field and number operators under two different types of non-Markovian noise models. We consider Ornstein-Uhlenbeck noise (OUN) and power-law noise (PLN), both of which have a well-defined Markovian limit. The time-dependent dephasing rates for these cases are given as [47,53]

$$\Gamma(t) = \begin{cases} \frac{\Gamma}{2}(1 - e^{-\lambda t}) & \text{for OUN} \\ \frac{\Gamma}{2(\lambda t+1)^3} & \text{for PLN,} \end{cases} \tag{19}$$

where Γ is the inverse relaxation time and λ and $1/\lambda$ are the noise bandwidths for OUN and PLN, respectively, which in turn are related to the finite correlation time of the environment. Note these quantities can be considered as the inverse environmental memory time that vanish in the limit of $\lambda \to \infty$ and $1/\lambda \to \infty$ for OUN and PLN, respectively, yielding the Markovian limits of these noise models. Naturally, in the Markovian limit, the time-dependent dephasing factors become time independent. It is important to note that in both cases $\Gamma(t)$ never becomes negative throughout the evolution. Therefore, the dynamics generated is completely positive (CP) divisible at all times and considered as Markovian [54,55]. Nevertheless, it is clear that finite environment correlation time results in non-Markovian behavior in the dynamics [44,47] such that any intermediate map taking the system from t_1 to t_2 is not independent of the initial time t_0. It has been shown that it is also possible to quantify these "weaker" forms of non-Markovianity emerging in these models, by adopting different strategies as shown in [53].

In [53] the authors provide a geometric measure of non-Markovianity that is capable of capturing the amount of non-Markovianity for the CP-divisible models considered above and provide a comparative analysis. Setting $x = \lambda^{-1}$ for OUN and $x = \lambda$ for PLN, it has been shown that the non-Markovianity of PLN is always higher than that of OUN for any finite x (cf. Fig. 1 of [53]). Note that $x = 0$ corresponds to the case $\lambda \to \infty$ for OUN and $1/\lambda \to \infty$ for PLN, which are the Markovian limits of these models. We set $x = 10$ and look at the noise-assisted transport phenomenon in a Glauber-Fock oscillator (lattice) under OUN and PLN, together with their corresponding Markovian limit. Figure 4 shows that for this value $x = 10$, which corresponds to $\lambda = 0.1$ for OUN and $\lambda = 10$ for PLN, the noise-assisted transport phenomenon shows a higher enhancement over a broader range of dephasing in the case of PLN as compared to OUN, which also presents a higher non-Markovianity.

In Fig. 4(a) we show that the pure numerical calculation of the master equation (11) coincides (as expected) with the solution of Eq. (16), but the latter is significantly more straightforward to solve than the former. Interestingly, even when we do not consider correlations between sites, one can still observe the enhancement in noise-assisted transport in the non-Markovian case described by the master equation (15). This suggests that for the specific model of GF oscillator (lattice) considered in this work, non-Markovianity seems quite advantageous in the noise-assisted transport phenomenon. Increased non-Markovianity in the open system dynamics allows us to achieve finite $\langle \hat{n}(t) \rangle$, or equivalently $\langle \hat{n}(z) \rangle_{\text{class}}$, for larger values of the dephasing rate. Although our findings are limited to the models considered in this work, they are in accordance with recent results in the literature that show positive correlation between non-Markovianity and noise-assisted transport efficiencies [26,56,57].

VI. CONCLUSION

We have explored the conditions under which the master equation describing a driven quantum harmonic oscillator, interacting with an environment in a nondissipative way, is equivalent to the master equation describing light propagation in a dynamically disordered photonic lattice, the Glauber-Fock photonic lattice. One of these conditions is that the noise between different sites (waveguides) must be correlated. The second condition is to choose a number of waveguides such that the light does not reach the boundary where the sites corresponding to high number states lie. Further, we have shown that the noise-assisted energy transport phenomenon can be observed in this type of system and that it is possible to obtain analytical solutions for certain observables quantities, e.g., the average photon number. Using these solutions, we can readily predict the maximum amount of energy transferred between all the sites. This, in the Markovian scenario, occurs for decoherence rates comparable to the energy scale of the system. For the non-Markovian case, we found that the range of the dephasing rate, in which the noise-assisted transport occurs, is substantially larger. Our results are in good agreement with recent theoretical [56,57] and experimental [26] works showing that non-Markovian environments have a strong influence on the energy transport. Looking forward, and following the ideas of Refs. [35,58], it would be interesting to go beyond the single-excitation regime and derive the corresponding master equation of, for example, two correlated particles propagating over these stochastic networks affected by non-Markovian noise.

APPENDIX A

The time derivative of the density matrix $\sigma_{nm}(t) \equiv \langle \psi_n \psi_m^* \rangle$ is given as

$$\frac{d}{dt}\sigma_{nm} = \left\langle \psi_m^* \frac{d\psi_n}{dt} + \psi_n \frac{d\psi_m^*}{dt} \right\rangle, \tag{A1}$$

where each term can be calculated using the stochastic Schrödinger equation:

$$\psi_m^* \frac{d\psi_n}{dt} = -in\omega\psi_n\psi_m^* - in\phi_n(t)\psi_n\psi_m^* - i\sum_{j\neq n}\kappa_{nj}\psi_j\psi_m^*, \tag{A2a}$$

$$\psi_n \frac{d\psi_m^*}{dt} = +im\omega\psi_n\psi_m^* + im\phi_m(t)\psi_n\psi_m^* + i\sum_{j\neq m}\kappa_{jm}\psi_n\psi_j^*. \tag{A2b}$$

Performing the stochastic averaging procedure, these terms yield

$$\frac{d}{dt}\sigma_{nm} = -i(n\omega - m\omega)\sigma_{nm} - i\sum_{j\neq n}\kappa_{nj}\sigma_{jm} + i\sum_{j\neq m}\kappa_{jm}\sigma_{nj} - in\langle\psi_n\psi_m^*\phi_n(t)\rangle + im\langle\psi_n\psi_m^*\phi_m(t)\rangle. \tag{A3}$$

In particular, to obtain the stochastic averages in the last two terms of Eq. (A3), one needs to resort to Novikov's theorem [48]

$$\langle\psi_n\psi_m^*\phi_n(t)\rangle = \sum_p \int dt' \langle\phi_n(t)\phi_p(t')\rangle \left\langle \frac{\delta[\psi_n(t)\psi_m^*(t)]}{\delta\phi_p(t')} \right\rangle \tag{A4a}$$

$$= \sum_p \int dt' \Gamma\delta_{np}\delta(t-t') \left\langle \frac{\delta[\psi_n(t)\psi_m^*(t)]}{\delta\phi_p(t')} \right\rangle \tag{A4b}$$

$$= \frac{1}{2}\sum_p \Gamma\delta_{np} \left\langle \frac{\delta[\psi_n(t)\psi_m^*(t)]}{\delta\phi_p(t)} \right\rangle \tag{A4c}$$

$$= \frac{\Gamma}{2} \left\langle \frac{\delta[\psi_n(t)\psi_m^*(t)]}{\delta\phi_n(t)} \right\rangle, \tag{A4d}$$

where the operator $\delta/\delta\phi_p(t)$ stands for the functional derivative with respect to the stochastic process. Similarly, the second term can be found as

$$\langle\psi_n\psi_m^*\phi_m(t)\rangle = \frac{\Gamma}{2} \left\langle \frac{\delta[\psi_n(t)\psi_m^*(t)]}{\delta\phi_m(t)} \right\rangle. \tag{A5}$$

To obtain Eqs. (A4c) and (A5) we have used the fact that, in the Stratonovich interpretation, $\int \delta(t) = \frac{1}{2}$ [59]. It is important to mention that Novikov's theorem is only valid for stochastic Gaussian processes, which can be either Markovian or non-Markovian as well [60]. To compute the corresponding functional derivatives we need the formal integration of Eq. (A3), which before the stochastic average is

$$\psi_n(t)\psi_m^*(t) = \int_0^t dt' [f(\psi_n\psi_m^*, \dots) - in\psi_n\psi_m^*\phi_n(t') + im\psi_n\psi_m^*\phi_m(t')], \tag{A6}$$

where $f(\psi_n\psi_m^*, \dots)$ represents all the terms that do not contain the stochastic variable $\phi_n(t)$. Thus, the functional derivatives are

$$\frac{\delta[\psi_n(t)\psi_m^*(t)]}{\delta\phi_n(t)} = -in\psi_n\psi_m^* + im\psi_n\psi_m^*\delta_{nm}, \tag{A7a}$$

$$\frac{\delta[\psi_n(t)\psi_m^*(t)]}{\delta\phi_m(t)} = -in\psi_n\psi_m^*\delta_{nm} + im\psi_n\psi_m^*, \tag{A7b}$$

in which we have used the identity $\delta\phi_p(t')/\delta\phi_q(t) = \delta_{pq}\delta(t'-t)$ [48]. Using these results, we can compute the stochastic average for the last two terms in Eq. (A3) as

$$-in\langle\psi_n\psi_m^*\phi_n(t)\rangle = -\tfrac{1}{2}\Gamma n^2\rho_{nm} + \tfrac{1}{2}\Gamma nm\rho_{nm}\delta_{nm}, \tag{A8a}$$

$$im\langle\psi_n\psi_m^*\phi_m(t)\rangle = \tfrac{1}{2}\Gamma nm\rho_{nm}\delta_{nm} - \tfrac{1}{2}\Gamma m^2\rho_{nm}, \tag{A8b}$$

and as a result we obtain Eq. (8).

APPENDIX B

Applying Novikov's theorem [48] in $\langle \psi_n \psi_m^* \Omega_n(t) \rangle$ we get

$$\langle \psi_n \psi_m^* \Omega_n(t) \rangle = \sum_p \int dt' \langle \Omega_n(t) \Omega_p(t') \rangle \left\langle \frac{\delta[\psi_n(t)\psi_m^*(t)]}{\delta \Omega_p(t')} \right\rangle \tag{B1a}$$

$$= \sum_p \int dt' \frac{\Gamma \lambda}{2} \delta_{np} e^{-\lambda|t-t'|} \left\langle \frac{\delta[\psi_n(t)\psi_m^*(t)]}{\delta \Omega_p(t')} \right\rangle. \tag{B1b}$$

The final aim of this Appendix is to know if the master equation (13), after applying Novikov's theorem in Eq. (B1b), will be similar to the master equation (11). Using the formal integration of Eq. (13), before doing the stochastic average, we can compute the functional derivative of Eq. (B1b) as

$$\frac{\delta[\psi_n(t)\psi_m^*(t)]}{\delta \Omega_p(t')} = \frac{\delta}{\delta \Omega_p(t')} \int_0^t dt'' [f(\psi_n \psi_m^*, \dots) - i n \psi_n \psi_m^* \Omega_n(t'') + i m \psi_n \psi_m^* \Omega_m(t'')]$$

$$= \int_0^t dt'' \left[-i n \psi_n \psi_m^* \frac{\delta \Omega_n(t'')}{\delta \Omega_p(t')} + i m \psi_n \psi_m^* \frac{\delta \Omega_m(t'')}{\delta \Omega_p(t')} \right]$$

$$= \int_0^t dt'' [-i n \psi_n \psi_m^* \delta_{np} \delta(t'' - t') + i m \psi_n \psi_m^* \delta_{mp} \delta(t'' - t')]$$

$$= -\frac{i}{2} n \psi_n(t') \psi_m^*(t') \delta_{np} + \frac{i}{2} m \psi_n(t') \psi_m^*(t') \delta_{mp}. \tag{B2}$$

Performing the stochastic average in Eq. (B2), we obtain

$$\left\langle \frac{\delta[\psi_n(t)\psi_m^*(t')]}{\delta \Omega_p(t')} \right\rangle = -\frac{i}{2} n \delta_{np} \sigma_{nm}(t') + \frac{i}{2} m \delta_{mp} \sigma_{nm}(t'). \tag{B3}$$

Now we substitute Eq. (B3) in Eq. (B1b),

$$\langle \psi_n \psi_m^* \Omega_n(t) \rangle = \sum_p \int dt' \frac{\Gamma \lambda}{2} \delta_{np} e^{-\lambda|t-t'|} \left\{ -\frac{i}{2} n \delta_{np} \sigma_{nm}(t') + \frac{i}{2} m \delta_{mp} \sigma_{nm}(t') \right\} \tag{B4a}$$

$$= -\frac{i}{2} n \int dt' \frac{\Gamma \lambda}{2} e^{-\lambda|t-t'|} \sigma_{nm}(t') + \frac{i}{2} m \delta_{mn} \int dt' \frac{\Gamma \lambda}{2} e^{-\lambda|t-t'|} \sigma_{nm}(t') \tag{B4b}$$

$$\approx -\frac{i}{2} n \sigma_{nm}(t) \int dt' \frac{\Gamma \lambda}{2} e^{-\lambda|t-t'|} + \frac{i}{2} m \delta_{mn} \sigma_{nm}(t) \int dt' \frac{\Gamma \lambda}{2} e^{-\lambda|t-t'|}, \tag{B4c}$$

where we have made an approximation $\sigma_{nm}(t') \approx \sigma_{nm}(t)$, i.e., we assume that the dynamics of the density matrix is slower compared with the dynamics of the stochastic processes. Under this approximation, we can perform the integral of Eqs. (B4),

$$\int_0^t dt' \frac{\Gamma \lambda}{2} e^{-\lambda|t-t'|} = \frac{\Gamma}{2} (1 - e^{-\lambda t}) \equiv \Gamma(t). \tag{B5}$$

With this result, Eq. (B4c) reduces to Eq. (14).

[1] S. Bose, Quantum Communication through an Unmodulated Spin Chain, Phys. Rev. Lett. **91**, 207901 (2003).

[2] M. Plenio and S. Huelga, Dephasing-assisted transport: Quantum networks and biomolecules, New J. Phys. **10**, 113019 (2008).

[3] P. Rebentrost, M. Mohseni, I. Kassal, S. Lloyd, and A. Aspuru-Guzik, Environment-assisted quantum transport, New J. Phys. **11**, 033003 (2009).

[4] G. Kurizki, P. Bertet, Y. Kubo, K. Mølmer, D. Petrosyan, P. Rabl, and J. Schmiedmayer, Quantum technologies with hybrid systems, Proc. Natl. Acad. Sci. U.S.A. **112**, 3866 (2015).

[5] M. O. Scully, K. R. Chapin, K. E. Dorfman, M. B. Kim, and A. Svidzinsky, Quantum heat engine power can be increased

by noise-induced coherence, Proc. Natl. Acad. Sci. U.S.A. **108**, 15097 (2011).

[6] M. Pezzutto, M. Paternostro, and Y. Omar, An out-of-equilibrium non-Markovian quantum heat engine, Quantum Sci. Technol. **4**, 025002 (2019).

[7] R. Román-Ancheyta, B. Çakmak, and Ö. E. Müstecaplıoğlu, Spectral signatures of non-thermal baths in quantum thermalization, Quantum Sci. Technol. **5**, 015003 (2020).

[8] M. Salado-Mejía, R. Román-Ancheyta, F. Soto-Eguibar, and H. Moya-Cessa, Spectroscopy and critical quantum thermometry in the ultrastrong coupling regime, Quantum Sci. Technol. **6**, 025010 (2021).

[9] A. Szameit and S. Nolte, Discrete optics in femtosecond-laser-written photonic structures, J. Phys. B **43**, 163001 (2010).

[10] M. Gräfe, R. Heilmann, M. Lebugle, D. Guzman-Silva, A. Perez-Leija, and A. Szameit, Integrated photonic quantum walks, J. Opt. **18**, 103002 (2016).

[11] A. Perez-Leija, R. Keil, A. Kay, H. Moya-Cessa, S. Nolte, L.-C. Kwek, B. M. Rodríguez-Lara, A. Szameit, and D. N. Christodoulides, Coherent quantum transport in photonic lattices, Phys. Rev. A **87**, 012309 (2013).

[12] D. N. Biggerstaff, R. Heilmann, A. A. Zecevik, M. Gräfe, M. A. Broome, A. Fedrizzi, S. Nolte, A. Szameit, A. G. White, and I. Kassal, Enhancing coherent transport in a photonic network using controllable decoherence, Nat. Commun. **7**, 11282 (2016).

[13] É.-O. Bossé and L. Vinet, Coherent transport in photonic lattices: A survey of recent analytic results, SIGMA **13**, 074 (2017).

[14] J. L. O'Brien, A. Furusawa, and J. Vučković, Photonic quantum technologies, Nat. Photon. **3**, 687 (2009).

[15] J. Wang, F. Sciarrino, A. Laing, and M. G. Thompson, Integrated photonic quantum technologies, Nat. Photon. **14**, 273 (2020).

[16] M. Gräfe and A. Szameit, Integrated photonic quantum walks, J. Phys. B **53**, 073001 (2020).

[17] H.-P. Breuer and F. Petruccione, *The Theory of Open Quantum Systems* (Oxford University Press on Demand, Oxford, 2002).

[18] A. Perez-Leija, H. Moya-Cessa, A. Szameit, and D. N. Christodoulides, Glauber-Fock photonic lattices, Opt. Lett. **35**, 2409 (2010).

[19] A. Rai and D. G. Angelakis, Quantum light in Glauber-Fock photonic lattices, J. Opt. **21**, 065201 (2019).

[20] R. Keil, A. Perez-Leija, F. Dreisow, M. Heinrich, H. Moya-Cessa, S. Nolte, D. N. Christodoulides, and A. Szameit, Classical Analog of Displaced Fock States and Quantum Correlations in Glauber-Fock Photonic Lattices, Phys. Rev. Lett. **107**, 103601 (2011).

[21] R. Keil, A. Perez-Leija, P. Aleahmad, H. Moya-Cessa, S. Nolte, D. N. Christodoulides, and A. Szameit, Observation of Bloch-like revivals in semi-infinite Glauber-Fock photonic lattices, Opt. Lett. **37**, 3801 (2012).

[22] A. J. Martínez, U. Naether, A. Szameit, and R. A. Vicencio, Nonlinear localized modes in Glauber-Fock photonic lattices, Opt. Lett. **37**, 1865 (2012).

[23] C. Yuce and H. Ramezani, Diffraction-free beam propagation at the exceptional point of non-Hermitian Glauber Fock lattices, arXiv:2009.12880.

[24] Z. Oztas, Nondiffracting wave beams in non-Hermitian Glauber-Fock lattice, Phys. Lett. A **382**, 1190 (2018).

[25] F. Caruso, A. Crespi, A. G. Ciriolo, F. Sciarrino, and R. Osellame, Fast escape of a quantum walker from an integrated photonic maze, Nat. Commun. **7**, 11682 (2016).

[26] C. Maier, T. Brydges, P. Jurcevic, N. Trautmann, C. Hempel, B. P. Lanyon, P. Hauke, R. Blatt, and C. F. Roos, Environment-Assisted Quantum Transport in a 10-Qubit Network, Phys. Rev. Lett. **122**, 050501 (2019).

[27] R. de J. León-Montiel, M. A. Quiroz-Juárez, R. Quintero-Torres, J. L. Domínguez-Juárez, H. M. Moya-Cessa, J. P. Torres, and J. L. Aragón, Noise-assisted energy transport in electrical oscillator networks with off-diagonal dynamical disorder, Sci. Rep. **5**, 17339 (2015).

[28] S. Viciani, M. Lima, M. Bellini, and F. Caruso, Observation of Noise-Assisted Transport in an All-Optical Cavity-Based Network, Phys. Rev. Lett. **115**, 083601 (2015).

[29] I. Kassal, J. Yuen-Zhou, and S. Rahimi-Keshari, Does coherence enhance transport in photosynthesis? J. Phys. Chem. Lett. **4**, 362 (2013).

[30] L. O. Castaños and A. Zuñiga-Segundo, The forced harmonic oscillator: Coherent states and the RWA, Am. J. Phys. **87**, 815 (2019).

[31] R. Román-Ancheyta, I. Ramos-Prieto, A. Perez-Leija, K. Busch, and R. de J. León-Montiel, Dynamical Casimir effect in stochastic systems: Photon harvesting through noise, Phys. Rev. A **96**, 032501 (2017).

[32] S. Stützer, A. S. Solntsev, S. Nolte, A. A. Sukhorukov, and A. Szameit, Observation of Bloch oscillations with a threshold, APL Photon. **2**, 051302 (2017).

[33] H. J. Carmichael, in *Statistical Methods in Quantum Optics 1: Master Equations and Fokker-Planck Equations*, edited by H. J. Carmichael, Texts and Monographs in Physics (Springer, Berlin, 1999), pp. 29–74.

[34] A. Perez-Leija, D. Guzmán-Silva, R. de J. León-Montiel, M. Gräfe, M. Heinrich, H. Moya-Cessa, K. Busch, and A. Szameit, Endurance of quantum coherence due to particle indistinguishability in noisy quantum networks, npj Quantum Inf. **4**, 45 (2018).

[35] R. de J. León-Montiel, V. Méndez, M. A Quiroz-Juárez, A. Ortega, L. Benet, A. Perez-Leija, and K. Busch, Two-particle quantum correlations in stochastically-coupled networks, New J. Phys. **21**, 053041 (2019).

[36] C. Navarrete-Benlloch, Open systems dynamics: Simulating master equations in the computer, arXiv:1504.05266.

[37] H. E. Kondakci, L. Martin, R. Keil, A. Perez-Leija, A. Szameit, A. F. Abouraddy, D. N. Christodoulides, and B. E. A. Saleh, Hanbury Brown and Twiss anticorrelation in disordered photonic lattices, Phys. Rev. A **94**, 021804(R) (2016).

[38] L. Martin, G. D. Giuseppe, A. Perez-Leija, R. Keil, F. Dreisow, M. Heinrich, S. Nolte, A. Szameit, A. F. Abouraddy, D. N. Christodoulides, and B. E. A. Saleh, Anderson localization in optical waveguide arrays with off-diagonal coupling disorder, Opt. Express **19**, 13636 (2011).

[39] S. Stützer, Y. V. Kartashov, V. A. Vysloukh, V. V. Konotop, S. Nolte, L. Torner, and A. Szameit, Hybrid Bloch-Anderson localization of light, Opt. Lett. **38**, 1488 (2013).

[40] F. Dreisow, A. Szameit, M. Heinrich, T. Pertsch, S. Nolte, A. Tünnermann, and S. Longhi, Bloch-Zener Oscillations in Binary Superlattices, Phys. Rev. Lett. **102**, 076802 (2009).

[41] M. A. Quiroz-Juárez, C. You, J. Carrillo-Martínez, D. Montiel-Álvarez, J. L. Aragón, O. S. Magaña Loaiza, and R. de J. León-Montiel, Reconfigurable network for quantum transport simulations, Phys. Rev. Research **3**, 013010 (2021).

[42] R. de J. León-Montiel and P. A. Quinto-Su, Noise-enabled optical ratchets, Sci. Rep. **7**, 44287 (2017).

[43] M. G. Sánchez-Sánchez, R. de J. León-Montiel, and P. A. Quinto-Su, Phase Dependent Vectorial Current Control in Symmetric Noisy Optical Ratchets, Phys. Rev. Lett. **123**, 170601 (2019).

[44] T. Yu and J. H. Eberly, Entanglement evolution in a non-Markovian environment, Opt. Commun. **283**, 676 (2010).

[45] C. Addis, B. Bylicka, D. Chruściński, and S. Maniscalco, Comparative study of non-Markovianity measures in exactly solvable one- and two-qubit models, Phys. Rev. A **90**, 052103 (2014).

[46] M. J. W. Hall, J. D. Cresser, L. Li, and E. Andersson, Canonical form of master equations and characterization of non-Markovianity, Phys. Rev. A **89**, 042120 (2014).

[47] N. P. Kumar, S. Banerjee, R. Srikanth, V. Jagadish, and F. Petruccione, Non-Markovian evolution: A quantum walk perspective, Open Syst. Inf. Dyn. **25**, 1850014 (2018).

[48] E. A. Novikov, Functionals and the random-force method in turbulence theory, J. Expt. Theor. Phys. (U.S.S.R.) **47**, 1919 (1964) [Sov. Phys. JETP **20**, 1290 (1965)].

[49] R. de J. León-Montiel and J. P. Torres, Highly Efficient Noise-Assisted Energy Transport in Classical Oscillator Systems, Phys. Rev. Lett. **110**, 218101 (2013).

[50] H. Fröml, A. Chiocchetta, C. Kollath, and S. Diehl, Fluctuation-Induced Quantum Zeno Effect, Phys. Rev. Lett. **122**, 040402 (2019).

[51] B. Misra and E. C. G. Sudarshan, The Zeno's paradox in quantum theory, J. Math. Phys. **18**, 756 (1977).

[52] T. Pertsch, P. Dannberg, W. Elflein, A. Bräuer, and F. Lederer, Optical Bloch Oscillations in Temperature Tuned Waveguide Arrays, Phys. Rev. Lett. **83**, 4752 (1999).

[53] S. Utagi, R. Srikanth, and S. Banerjee, Temporal self-similarity of quantum dynamical maps as a concept of memorylessness, Sci. Rep. **10**, 15049 (2020).

[54] Á. Rivas, S. F Huelga, and M. B Plenio, Quantum non-Markovianity: Characterization, quantification and detection, Rep. Prog. Phys. **77**, 094001 (2014).

[55] H.-P. Breuer, E.-M. Laine, J. Piilo, and B. Vacchini, Colloquium: Non-Markovian dynamics in open quantum systems, Rev. Mod. Phys. **88**, 021002 (2016).

[56] N. Trautmann and P. Hauke, Trapped-ion quantum simulation of excitation transport: Disordered, noisy, and long-range connected quantum networks, Phys. Rev. A **97**, 023606 (2018).

[57] S. V. Moreira, B. Marques, R. R. Paiva, L. S. Cruz, D. O. Soares-Pinto, and F. L. Semião, Enhancing quantum transport efficiency by tuning non-Markovian dephasing, Phys. Rev. A **101**, 012123 (2020).

[58] A. Perez-Leija, R. de J. Leon-Montiel, J. Sperling, H. Moya-Cessa, A. Szameit, and K. Busch, Two-particle four-point correlations in dynamically disordered tight-binding networks, J. Phys. B **51**, 024002 (2017).

[59] N. G. van Kampen, Itô versus Stratonovich, J. Stat. Phys. **24**, 175 (1981).

[60] W. T. Strunz and T. Yu, Convolutionless non-Markovian master equations and quantum trajectories: Brownian motion, Phys. Rev. A **69**, 052115 (2004).